Autofluorescence Lifetimes in Patients With Choroideremia Identify Photoreceptors in Areas With Retinal Pigment Epithelium Atrophy

Chantal Dysli,[1] Sebastian Wolf,[1] Hoai Viet Tran,[2] and Martin S. Zinkernagel[1]

[1]Departments of Ophthalmology and Clinical Research, Inselspital, Bern University Hospital, University of Bern, Switzerland
[2]Department of Ophthalmology, Jules-Gonin Eye Hospital, University of Lausanne, Lausanne, Switzerland

Correspondence: Martin S. Zinkernagel, University Hospital Bern, 3010 Bern, Switzerland; m.zinkernagel@gmail.com.

Submitted: July 25, 2016
Accepted: October 24, 2016

Citation: Dysli C, Wolf S, Tran HV, Zinkernagel MS. Autofluorescence lifetimes in patients with choroideremia identify photoreceptors in areas with retinal pigment epithelium atrophy. *Invest Ophthalmol Vis Sci*. 2016;57:6714–6721. DOI:10.1167/iovs.16-20392

Purpose. The purpose of this study was to investigate fundus autofluorescence lifetimes in patients with choroideremia and to identify tissue-specific lifetime characteristics and potential prognostic markers.

Methods. Autofluorescence lifetimes of the retina were measured in two spectral channels (498–560 nm and 560–720 nm) in patients with choroideremia and age-matched healthy controls. Furthermore, autofluorescence intensities and spectral-domain optical coherence tomography (OCT) data were acquired and compared to fundus autofluorescence lifetime data.

Results. Sixteen eyes from 8 patients with advanced choroideremia (mean ± SD age, 55 ± 13 years) were included in this study and compared with 10 age-matched healthy participants. Whereas fundus autofluorescence intensity measurement identified areas of remaining retinal pigment epithelium (RPE), autofluorescence lifetime maps identified areas with remaining photoreceptor layers in OCT but RPE atrophy. In these areas, mean (±SEM) lifetimes were 567 ± 59 ps in the short and 603 ± 49 ps in the long spectral channels (+98% and +88% compared to controls). In areas of combined RPE atrophy and loss of photoreceptors, autofluorescence lifetimes were significantly prolonged by 1116 ± 63 ps (+364%) in the short and by 915 ± 52 ps (+270%) in the long spectral channels compared with controls.

Conclusions. Because autofluorescence lifetimes identify areas of remaining photoreceptors in the absence of RPE, this imaging modality may be useful to monitor disease progression in the natural course of disease and in context of potential future therapeutic interventions.

Keywords: choroideremia, FLIO, fluorescence lifetimes, fundus autofluorescence, retinal dystrophies, retinal imaging

Choroideremia (CHM) is a rare hereditary retinal disease leading to progressive degeneration of the choroid, the retinal pigment epithelium (RPE), and the retina due to a mutation of the CHM gene located on the X chromosome. Because of its X-linked inheritance pattern, CHM primarily affects male subjects with an estimated prevalence of approximately 1:50,000, but female patients may be affected in a mosaic disease pattern.[1–3] The CHM gene (*Xq21.2*) encodes a ubiquitously expressed protein (Rab escort protein [*REP-1*]) which enables posttranslational modification of Rab proteins. This protein modification pathway is essential for intracellular vesicular and membrane trafficking pathways.[2] Systemically, no other effects of the deficient *REP-1* is observed because the autosomal inherited *REP-2* can compensate for the deficient *REP-1*.[3]

CHM is diagnosed clinically by the typical fundus appearance and the inheritance pattern and can be confirmed by genetic analysis.[1] Patients typically report onset of night blindness during the first decade followed by progressive loss of peripheral vision. Due to the slow progression of disease, the central fovea is often preserved until late disease stages (50 to 70 years of age). Finally, CHM can result in total blindness when all remaining photoreceptors—RPE—island complexes have degenerated.[1] The ocular fundus typically has a pale appearance due to the exposure of the underlying sclera after progressive loss of the outer retina, the RPE and the choroidal vessels.[4] Typically, the remaining islands with preserved RPE appear as areas with normal or increased autofluorescence intensity due to lipofuscin accumulation, whereas areas with RPE atrophy are characterized by hypoautofluorescence.[1,5]

Whereas fundus autofluorescence intensity is a good indicator for lipofuscin content and thus RPE integrity, fundus autofluorescence lifetime imaging is a relatively novel technique in clinical use for noninvasive identification and quantification of specific metabolic conditions within the retina in different retinal diseases.[6–10] The method is based on preliminary work of Schweitzer et al.,[11–13] who adapted the technique for in vivo measurement in the human eye. The fluorescence lifetime describes the time span a natural retinal fluorophore spends at its higher energy level after excitation with a blue laser light before it returns to its ground level of energy under emission of autofluorescence.

In this study, we analyzed fundus autofluorescence lifetimes in patients with CHM and investigated potential changes of fluorescence lifetimes during follow-up examinations.

Table 1. Patient Characteristics

Patient	Sex	Age	Age at Initial Diagnosis	ETDRS Visual Acuity		Area of RPE, mm²		Follow-Up, Months	
				Right	Left	Right	Left	Number	Duration
CHM1	M	51	Child	64	84	3.96	6.04	4	27
CHM2	M	44	Child	82	78	26.03	24.2	6	39
CHM3	M	70	33	66	66	1.23	0.69	–	–
CHM4	M	51	Child	33	83	0.36	1.4	1	11
CHM5	M	64	30	65	LP*	1.06	0.64	1	12
CHM6	M	32	30	61	75	1.57	1.24	–	–
CHM7	M	68	53	60	LP*	0.59	1.72	–	–
CHM8	M	56	45	3	64	1.3	1.58	–	–

* LP, light perception.

Methods

This prospective study was performed with the approval of the local ethics committee and was carried out in accordance with the International Ethical Guidelines for Biomedical Research involving Human Subjects (Council for International Organizations of Medical Sciences). It is registered at ClinicalTrials.gov (NCT01981148) under the title Measurement of Retinal Autofluorescence with a Fluorescence Lifetime Imaging Ophthalmoscope. All participants were recruited at the outpatient department at the University Hospital of Bern, Switzerland, and signed informed consent prior to study entry.

Subjects and Procedures

At every visit, both eyes were investigated. For all study participants, best corrected visual acuity (using Early Treatment Diabetic Retinopathy Study [ETDRS] letters)[14] and noncontact intraocular pressure (air tonometry) were assessed. A general ophthalmic examination after maximal pupil dilation using tropicamide, 0.5%, and phenylephrine hydrochloride, 2.5%, was performed to exclude other ophthalmic conditions such as media opacities that might have interfered with multimodal imaging. The diagnosis of CHM was confirmed by at least two independent retinal specialists and was based on the typical fundus appearance, autofluorescence and optical coherence tomography (OCT) imaging, and family history. Gene mutations included CHM (*REP-1*): c.[16-17dup](p.S7Lfs*6) exon 1 in one patient and CHM (RNA): Allele 1: c.[1770+520C>G], p.[A591_*654delinsQMNQ*], Allele 2: [0] in two patients (cousins). All participants underwent multimodal imaging at every visit with fundus color imaging (FF 450plus camera; Zeiss, Oberkochen, Germany), OCT, and autofluorescence (FAF) intensity measurement of the macula (Spectralis HRA+OCT; Heidelberg Engineering, Heidelberg, Germany), and fluorescence lifetime imaging ophthalmoscopy (Heidelberg Engineering).

Fluorescence Lifetime Imaging Ophthalmoscope

The fluorescence lifetime imaging ophthalmoscope is based on a Heidelberg retina angiograph (HRA) Spectralis system (Heidelberg Engineering). A 473-nm pulsed laser, raster scanning of the central fundus with a repetition rate of 80 MHz was used for excitation of retinal autofluorescence.

The total scan duration per eye lasted approximately 90 seconds. A built-in infrared reflectance camera tracks eye movements and ensures that every fluorescence photon emitted is recorded at the correct spatial location. These photons are detected by highly sensitive hybrid photon-counting detectors (HPM-100-40; Becker & Hickl, Berlin, Germany) in a short spectral channel (SSC, 498–560) and in a long spectral channel (LSC, 560–720) and registered by time-correlated single-photon counting modules (SPC-150; Becker & Hickl).

Recorded fluorescence lifetime data were analyzed separately within the SSC and LSC using SPCImage 4.6 software (Becker & Hickl). For every location within the 256 × 256-pixel grid covering the central 30° of the macula, a decay trace was built from the recorded single photons, and a bi-exponential decay function was calculated using a binning factor of 1.

The mean fluorescence lifetime tau mean (*Tm*) represents the amplitude weighted mean fluorescence decay time per pixel and wavelength channel.

$$Tm = \frac{\alpha 1 * T1 + \alpha 2 * T2}{\alpha 1 + \alpha 2} \quad (1)$$

Tm for every pixel within the SSC and the LSC consists of a short decay component, *T1*, with its relative amplitude (equal to relative intensity), *α1*, and a long decay component, *T2*, with its relative amplitude, *α2*, whereby $T1 << T2$ and $\alpha 1 >> \alpha 2$ ($\alpha 1$ = approximately 90%; range, 96% [macular center]–80% [periphery]; $\alpha 2$ = approximately 10%; range, 4%–20%).

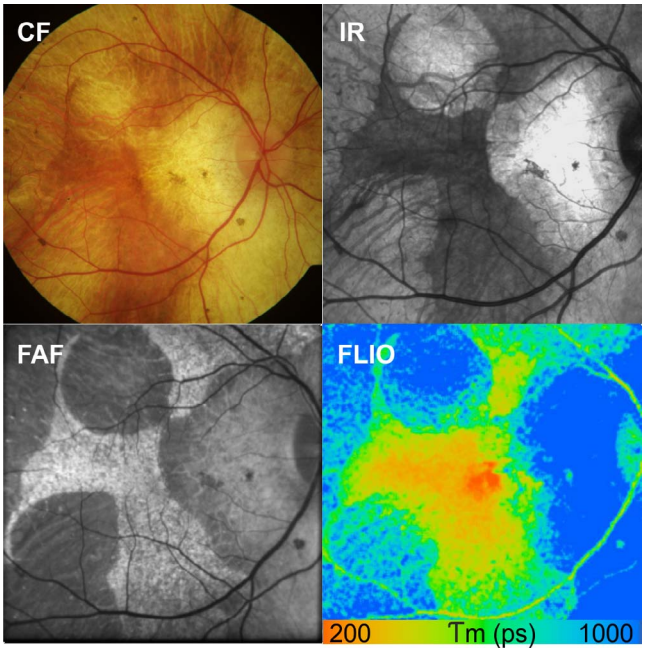

Figure 1. Representative fundus autofluorescence lifetime measurement of a patient with CHM. Multimodal imaging with corresponding CF, IR, FAF intensity, and autofluorescence lifetime images is shown (CHM patient 2). FLIO SSC, 498 to 560 nm; color scale, 200 to 1000 ps.

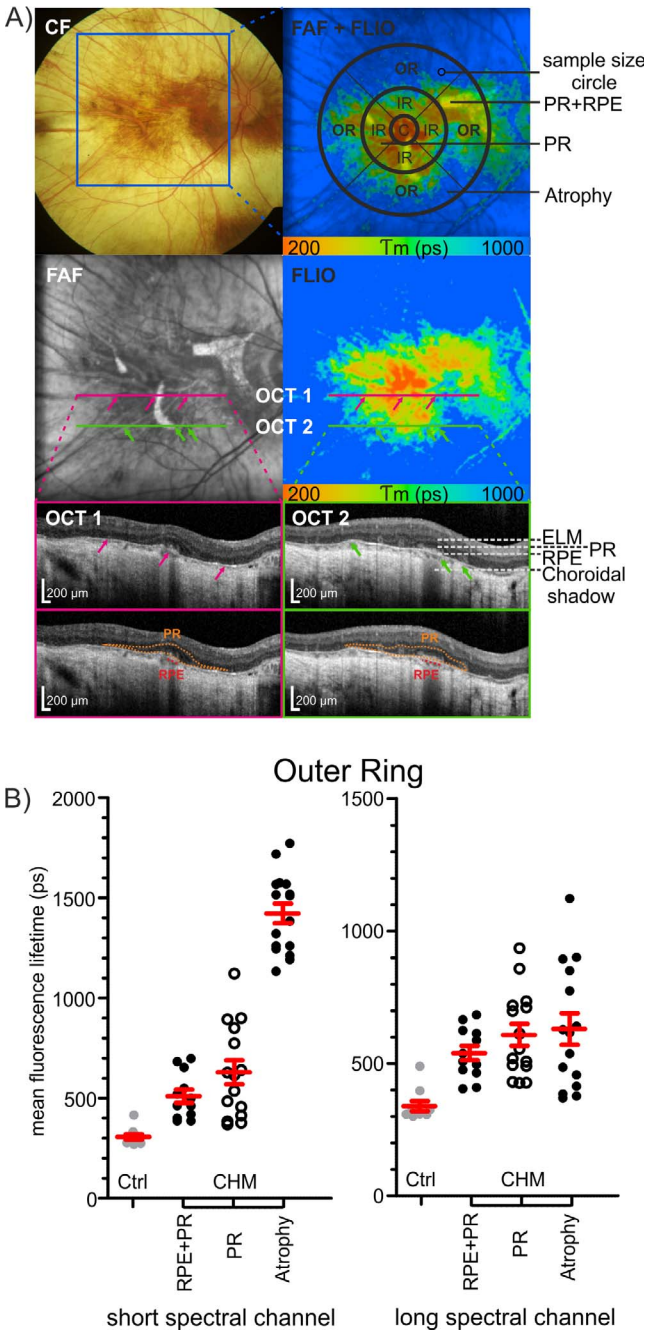

Figure 2. Quantitative analysis of retinal autofluorescence lifetimes in CHM and correlation with optical coherence tomography findings. (**A**) Color fundus, FAF intensity, and autofluorescence lifetime image (SSC color range, 200–1000 ps) of a 51-year-old male (CHM patient 4) are shown. The *right upper* image shows an overlay of FAF and FLIO with the indicated analysis method. Mean fluorescence lifetime values were averaged for the ETDRS grid *center* (diameter [*d*] = 1 mm) and the *inner* (*d* = 3 mm) and the *outer* (*d* = 6 mm) ETDRS ring. The indicated sample size circle (*d* = 0.2mm) was used for analysis of specific regions. The *purple* and *green* bars represent OCT scan lines of the OCT scans below (OCT 1 = *purple*, *left side*; OCT 2 = *green*, *right side*). Corresponding points are marked with *arrows* of the same color (*purple* or *green*) within FAF, FLIO, and OCT. The external limiting membrane (ELM), remaining photoreceptors (PR), and retinal pigment epithelium (RPE) are marked in OCT scan 2. Areas of intact RPE (*red* [*shadowing* of the choroid below]) and areas with remaining PR (*orange*) are marked in the lowest OCT. (**B**) Mean fluorescence lifetime values in specific areas of analysis within the outer ring of the ETDRS grid. RPE+PR, area of intact RPE, PR and normal retinal layer structure. PR, area without RPE but remaining photoreceptor and choroidal cell layer. Atrophy, area with complete chorioretinal atrophy. Data are shown for the short (498–560 nm) and long (560–720 nm) spectral channel for CHM patients and compared with age-matched healthy controls (ctrl [*gray dots*]). *n* = 16 CHM eyes and *n* = 10 control subjects. Each data point represents a mean value of three sample locations (*d* = 0.2 mm) within the corresponding area.

The technical background of the fluorescence lifetime imaging (FLIO) system as well as the extensive laser safety calculations provided by Heidelberg Engineering, according to the International Electrotechnical Commission,[15] have been described previously.[7,16]

Optical Coherence Tomography Analysis

Findings in color fundus images, FAF, and FLIO were compared and correlated with measurements on OCT scans. Retinal pigment epithelium atrophy was defined when enhanced choroidal signal was present and/or a disruption of the RPE was visible.

Fluorescence Intensity Data Analysis

Areas with high autofluorescence intensity, corresponding to remaining islands of retinal pigment epithelium, were marked manually, using the region overlay device of the Heidelberg Eye Explorer software.

Fluorescence Lifetime Data Analysis

The mean fluorescence lifetime *Tm*, the short *T1* and the long *T2* decay components with corresponding amplitudes $\alpha 1$ and $\alpha 2$ were further analyzed using custom-made "FLIO reader" (Artificial Organs Center for Biomedical Engineering Research, University of Bern, Bern, Switzerland). The FLIO reader builds mean values from the respective component within the fields of a standard ETDRS grid (a circle diameter of the central area of 1 mm; an inner ring of 3 mm; and an outer ring of 6 mm).[16] For further analysis, the grid size was adjusted as stated directly in the text. For measurement of specific areas within FLIO pictures, images were imported using ImageJ software (version 1.50i; http://imagej.nih.gov/ij/; provided in the public domain by the National Institutes of Health, Bethesda, MD, USA), and the borders were manually marked after calibration with a scaling factor.

Statistical Analysis

Mean ± standard errors of the mean (SEM) were calculated. Prism version 6 (GraphPad Software, Inc., La Jolla, CA, USA) was used for statistical data analysis. Parametric data were compared using 2-tailed Student's *t*-test with a confidence interval (CI) of 95%. To eliminate dependence of growth rates from baseline lesion size, a square root transformation was used to calculate the yearly progression factor[17]:

$$\sqrt{\frac{Follow\ up\ Area\ (mm^2)}{Baseline\ Area\ (mm^2)}} \qquad (2)$$

Results

Sixteen eyes of 8 patients with CHM were included in this study. The mean ± SD age was 55 ± 13 years (range, 32–70 years of age). All eyes but one were phakic, but there were no

Investigative Ophthalmology & Visual Science

Table 2. Fluorescence Lifetime Analysis in Specific Locations

	Center				Inner Ring				Outer Ring				
Spectral Channel	Control	RPE+PR	*P* Value	PR	Control	RPE+PR	*P* Value	PR	Control	RPE+PR	*P* Value	PR	Atrophy
Short spectral channel, 498–560 nm													
Mean	194.2	375.2	0.0002	498.3	286.9	490.7	<0.0001	567.3	306.2	510.2	<0.0001	629.6	1422
SEM	15.91	34.17		86.89	16.49	32.68		58.94	13.67	32.82		59.88	49.06
Coefficient of variation	25.89%	31.55%		55.15%	18.18%	24.92%		41.56%	14.11%	22.28%		36.83%	13.80%
Long spectral channel, 560–720 nm													
Mean	273.4	443.8	0.0001	551	322.6	521.7	<0.0001	602.6	338.4	539	<0.0001	607.6	1253
SEM	20.16	27.91		72.71	21.13	26.8		48.5	18.82	27.47		41.53	39.47
Coefficient of variation	23.31%	21.79%		43.76%	20.72%	19.22%		32.19%	17.58%	17.66%		26.47%	12.60%

RPE+PR, area of intact retinal pigment epithelium (RPE) and photoreceptors (PR) and normal retinal layer structure. PR, area without retinal pigment epithelium but remaining photoreceptor and choroidal cell layer. Atrophy, area with complete chorioretinal atrophy.

Figure 3. Correlation of retinal thickness with autofluorescence lifetimes and optical coherence tomography. Islands of retinal pigment epithelium (RPE [*red dotted lines*]) are marked within FAF intensity images and remaining photoreceptors (*orange dashed lines*) are detectable using autofluorescence lifetime imaging (FLIO [SSC]; CHM patient 1). The two outlines then were superimposed in both the FLIO and FAF images. The findings are validated on representative OCT slices from indicated lines. Corresponding areas are marked with a *red dotted line* for the border of the RPE island and with an *orange dotted line* for the area with remaining photoreceptors. CF, color fundus; IR, infrared.

significant lens opacities. Typical fundus appearance of CHM with remaining small RPE islands was present in all included eyes. Ten age-matched healthy phakic subjects without significant lens opacities served as controls (mean ± SD age: 53 ± 9 years; range, 38–70 years of age; $P = 0.79$). Patients' characteristics, visual acuity, and morphologic data are summarized in Table 1.

A representative overview of multimodal imaging performed in patients with CHM including color fundus, infrared images, OCT, FAF, and FLIO, is shown in Figure 1. The mean size of areas with bright fundus autofluorescence (remaining RPE) was 4.6 ± 2 mm^2 (mean ± SEM) at baseline (range, 0.36–26 mm^2).

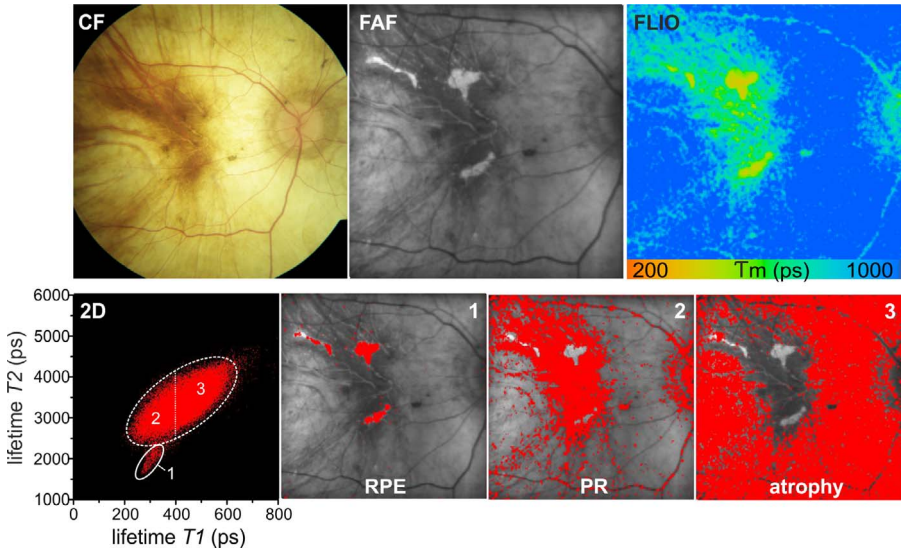

Figure 4. Analysis of individual lifetime components and spatial distribution in patients with CHM. Color fundus, FAF intensity, and mean fluorescence lifetime (*Tm* [LSC]) images (CHM patient 8). Corresponding distribution histograms of the short decay component *T1* versus the long decay component *T2* (Equation 1) are shown. Spatial distribution of different lifetime clusters as follows: (1) retinal pigment epithelium with short *T1* and short *T2*: (2) photoreceptors with short *T1* and midrange *T2*; and (3) chorioretinal atrophy with long *T1* and long *T2*.

The mean autofluorescence lifetime within specific regions of interest are summarized in Figure 2 and Table 2.

Fluorescence Lifetimes in Areas of Intact RPE and Outer Retinal Layers

In a first step, we analyzed differences between autofluorescence lifetimes between patients with CHM and healthy participants within areas of intact RPE identified by preserved autofluorescence intensity. As in healthy subjects, the shortest fluorescence lifetimes were generally seen within the macula, probably originating from macular pigment.[9] When we compared mean fluorescence lifetimes from the central subfield of the ETDRS grid of CHM patients with those of healthy age-matched controls, *Tm* was prolonged by 93% in the SSC (498–560 nm) ($P = 0.0002$) and by 62% in the LSC (560–720 nm) ($P = 0.0001$). In the area of the inner ETDRS ring, the differences were 71% and 62% in the SSC and the LSC, respectively, and 67% and 59% in the outer ETDRS ring, respectively (all $P < 0.0001$).

Fluorescence Lifetimes in Areas of Chorioretinal Atrophy

Areas of chorioretinal atrophy identified by hypoautofluorescence in FAF, choroidal signal enhancement, and absence of the outer nuclear layer in OCT showed a significantly prolonged *Tm* with 1422 ps (464% of control values) in the SSC and 1253 ps (370%) in the LSC compared to corresponding retinal areas in age-matched controls ($P < 0.0001$).

Fluorescence Lifetimes in Areas of RPE Atrophy but Remaining Outer Retinal Layers

Areas of relatively preserved fluorescence intensity in FAF images corresponded exactly to areas of intact RPE in OCT (Figs. 2, 3). However, these RPE borders were not directly identifiable within the *Tm* lifetime map. The outer borders of the areas with shorter autofluorescence lifetimes correlated to areas with remaining photoreceptor cell layer, independent of the presence or absence of the underlying RPE. The mean area of these islands with shorter lifetimes was 17.9 ± 3.3 mm^2 (range, 1.6–44.2 mm^2).

Autofluorescence lifetimes in areas with RPE atrophy but remaining photoreceptor layer in OCT were prolonged by 33% respectively, 24% in the central ETDRS area, by 16% in the inner ring, and by 23% respectively, 13% in the outer ring (SSC respectively, LSC) compared to corresponding retinal areas in age-matched controls. The FAF area-to-FLIO area ratio within the same eye showed a range of 1:1.8 to 1:77 (e.g., see Figs. 1–3).

Analysis of Individual Fluorescence Lifetime Components

For detailed analysis, the amplitude weighted mean fluorescence lifetime value *Tm* was divided into its single components *T1* (short decay component) and *T2* (long decay component). Data were visualized in a two-dimensional (2-D) dot plot with *T1* on the *x*-axis and *T2* on the *y*-axis (Fig. 4). In both the SSC and the LSC, the remaining retinal islands with intact RPE and PR featured a particularly short decay component *T2*. The surrounding retina was represented by one single lifetime cluster. Thereby, the area with remaining photoreceptor layer featured the shortest decay component *T1*, followed by the retinal vessels and the optic nerve head. The surrounding retina with bare choriosclera structures featured the longest *T2*, contributing to the long *Tm* values. In follow-up examinations, the lifetime cluster originating from the remaining RPE islands decreased (Fig. 5B).

Follow-up Examinations

Follow-up examinations of 50% of the eyes ($n = 8$) were performed with repetitive FLIO measurements up to 6 times over 3 years to assess disease-associated changes over time. In 8 eyes of 4 patients with CHM, a follow-up examination was performed after 1 year. Two patients were examined six times within the last 3 years. Even though there was no significant change in the assessed best visual acuity, all patients reported a slight decrease (and in one case, a severe reduction) of their vision within this period of time. Whereas retinal changes were

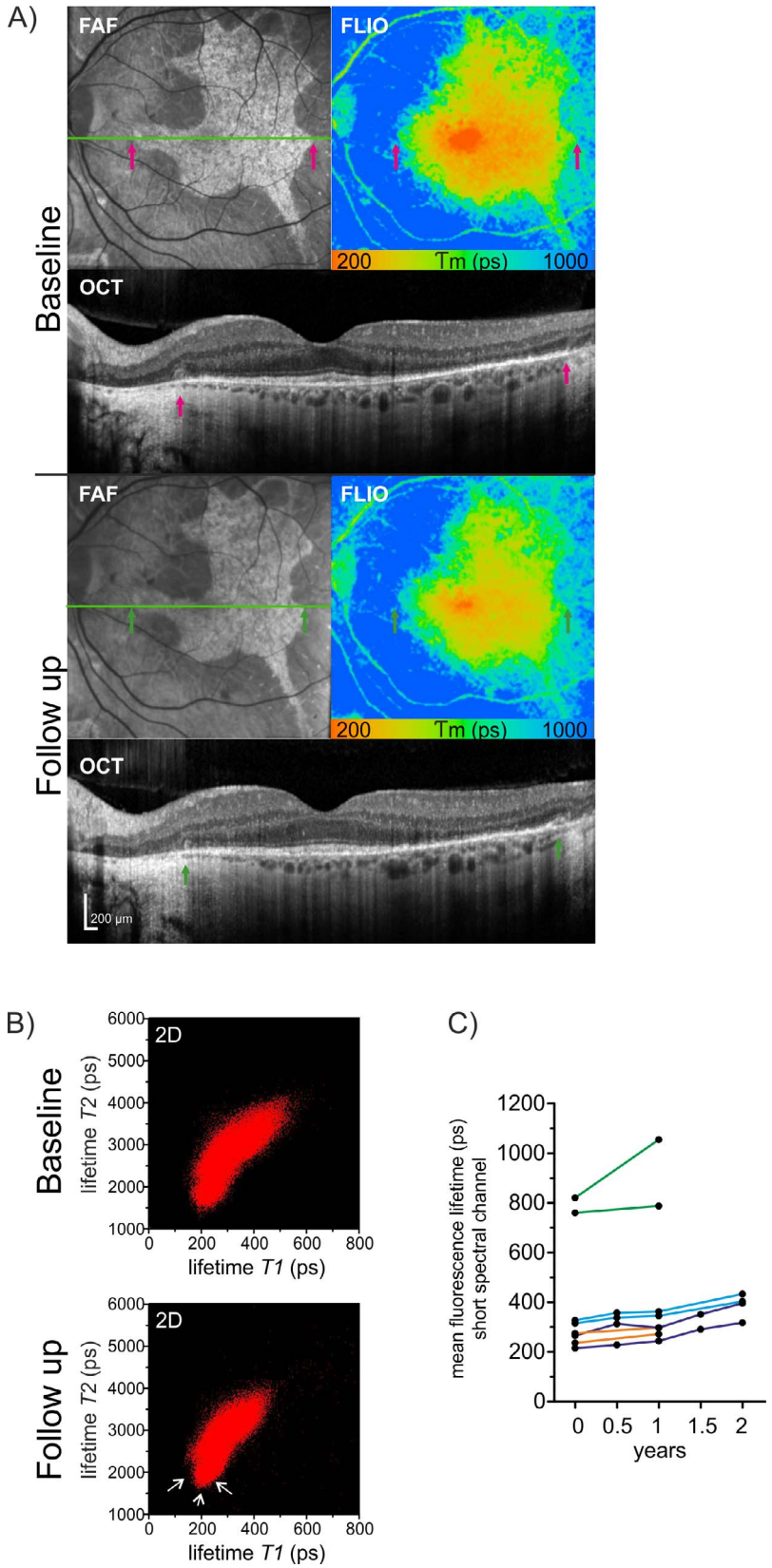

Figure 5. Longitudinal changes of fluorescence lifetimes in patients with CHM. Follow-up examinations with fluorescence lifetime imaging ophthalmoscopy (CHM patient 2). (**A**) Corresponding FAF intensity, FLIO (SSC) and OCT images are shown. Corresponding points are marked with *arrows* of the same color (*purple* or *green*) within FAF, FLIO, and OCT. A moderate reduction of the area with normal retinal pigment epithelium in the FAF image as well as the area of remaining photoreceptors, is mirrored by a decrease of short retinal fluorescence lifetimes in the FLIO image is shown. (**B**) Two-dimensional distribution histograms (*T1* versus *T2* [Equation 1]) are shown for the baseline as well as for the follow-up examination. There is a moderate reduction of the short lifetime cloud (*white arrows*). (**C**) A general prolongation of mean retinal autofluorescence lifetimes of the central area and the inner ring of the ETDRS grid is measured in the follow-up examinations ($n = 8$ eyes of 4 patients, one color per patient).

difficult to assess in color fundus images, in the FAF images, the outer border of the intact retinal islands were clearly discernible. Within 1 year, the mean area of intact retinal structure decreased by 7% (0.48 mm^2), with a range of 1.7% to 11.1% (0.04–1.73 mm^2). The area of short retinal fluorescence lifetimes decreased by 14% (3.4 mm^2). Square root transformation of the data according to Equation 2 revealed a mean decrease of 7.9% of the FAF area and 7.6% of the FLIO area. Over this observation period, *Tm* was prolonged by 56 ± 30 ps (14%) in the SSC and 8 ± 7 ps (1.5%) in the LSC within the central ETDRS circle (Fig. 5). There was an average extension of autofluorescence lifetimes of 36 ps/year in the RPE islands and 50 ps/year in areas with RPE atrophy but remaining photoreceptors and choroid in the SSC.

Discussion

In this report we showed that autofluorescence lifetimes originating from areas with remaining photoreceptor cell layers feature short decay times independent of the presence or absence of the underlying RPE. As such, additional information can be obtained on the state of photoreceptors in patients with CHM and may be helpful to further our understanding of the pathophysiology of this rare disease.

Although the underlying defect in CHM can be specifically attributed to a mutation within the gene that encodes *REP-1* with subsequent retinal degeneration, characteristically for CHM,[18] the exact pathomechanism of this hereditary disease has not yet been resolved. There is controversy about which layers are primarily affected by the disease and which undergo consecutive degeneration. Recently, wave front analysis using adaptive optics confirmed evidence from previous reports that the RPE is one primary site of degeneration in CHM.[18] In our current study using FLIO for measurement of autofluorescence lifetimes of the ocular fundus in CHM, we were able to identify areas with remaining photoreceptors in the absence of the RPE. A striking finding is that, in contrast to areas with photoreceptor atrophy which display very long fluorescence lifetimes, these areas feature short fluorescence lifetimes. Two findings associated with short fluorescence lifetimes merit further discussion. In the first instance, data from other studies[19] and from our previous studies[7] suggest that components of the visual cycle such as all-*trans* retinal (atRAL) display very short lifetimes. Under conditions of visual cycle dysfunction, retinoid cycle by-products have been shown to accumulate in outer segments of photoreceptor cells and the RPE.[20,21] Therefore, short autofluorescence lifetimes found in areas of remaining photoreceptors may indicate that there is some remaining activity of the visual cycle and generation of visual cycle by-products. This hypothesis is further supported by findings in a mouse model of retinal detachment where autofluorescence measurements revealed hyperfluorescent spots within the area of detached retina which were spectroscopically similar to the bisretinoids that constitute RPE lipofuscin.[22] This explanation for the short autofluorescence lifetimes observed in areas of RPE atrophy, but remaining photoreceptors are speculative but consistent with previous hypothesis on the pathophysiology of CHM.

On the other hand, recent data suggest that distinct patterns of short fluorescence lifetimes within the fovea derive from macular pigment.[9] In patients with CHM, macular pigment present in the plexiform layers and the photoreceptor axon layers in areas with RPE atrophy may therefore lead to short fluorescence lifetimes, at least in the fovea (Fig. 2). It was previously shown in a case series that macular pigment optical densities in patients with CHM do not differ from those in age-matched healthy controls.[23] Although we did not quantify this, this appears to be in keeping with our findings. However, in cases of advanced chorioretinal atrophy involving the center, such as seen in Figure 4, the area with short lifetimes disappears. Thus, the distribution of very short fluorescence lifetimes within the macular center may be used as a follow-up parameter and may serve as an indicator of the integrity of the Henle fiber layer and the outer plexiform layer containing the macular pigment.

However, even in areas with intact RPE verified by autofluorescence imaging, fluorescence lifetimes are already prolonged compared to corresponding areas in age-matched healthy controls. Accumulation of lipofuscin derivatives, which have been shown to display long lifetimes (1262 ps),[12,24] could explain our findings. This supports the hypothesis that the RPE might be the primary site of degeneration.[1] Additionally, loss of photoreceptors and concomitant decrease of visual cycle by-products may also lead to longer fluorescence lifetimes in areas with intact RPE. The latter is supported by adaptive optic findings with cone density loss in such areas of patchy RPE damage.[18] The information about RPE function and loss of photoreceptors in remaining RPE islands will be useful to assess disease activity and serve as control for future therapies in the field of gene therapy.[1,4,25]

The option to obtain information on individual lifetime components such as *T1* and *T2* and the corresponding amplitudes by 2D plotting of individual lifetime clusters allows visualization of the distinct aspects of disease progression over time and will be useful to monitor therapeutic approaches by quantifying changes in lifetime clusters over time as seen in Figure 5. Furthermore, FLIO could provide information about the location where to deliver the subretinal vector deposits: on one hand to not harm the remaining RPE and on the other hand having a higher chance to integrate in areas with still existing photoreceptor cell structures.

Conclusions

In vivo autofluorescence lifetime measurement can be used for tissue characterization in CHM. Remaining outer retinal layers correlate with short fluorescence lifetimes even in the absence of the retinal pigment epithelium. Prolongation of fluorescence lifetimes over time indicates disease progression and therefore might be used for follow-up of subtle retinal changes.

Acknowledgments

Supported by Swiss National Science Foundation 320030_156019.

Disclosure: **C. Dysli**, Heidelberg Engineering (S); **S. Wolf**, Heidelberg Engineering (C, S), Optos (C, F), Zeiss (C, F); **H.V. Tran**, None; **M.S. Zinkernagel**, Heidelberg Engineering (S)

References

1. Zinkernagel MS, MacLaren RE. Recent advances and future prospects in choroideremia. *Clin Ophthalmol*. 2015;9:2195–2200.
2. Kalatzis V, Hamel CP, MacDonald IM; for the First International Choroideremia Research Symposium. Choroideremia: towards a therapy. *Am J Ophthalmol*. 2013;156:433–437.
3. Zhang AY, Mysore N, Vali H, et al. Choroideremia is a systemic disease with lymphocyte crystals and plasma lipid and RBC membrane abnormalities. *Invest Ophthalmol Vis Sci*. 2015;56:8158–8165.
4. Barnard AR, Groppe M, MacLaren RE. Gene therapy for choroideremia using an adeno-associated viral (AAV) vector. *Cold Spring Harb Perspect Med*. 2015;5:a017293.

5. Syed R, Sundquist SM, Ratnam K, et al. High-resolution images of retinal structure in patients with choroideremia. *Invest Ophthalmol Vis Sci*. 2013;54:950–961.
6. Dysli C, Wolf S, Zinkernagel MS. Fluorescence lifetime imaging in retinal artery occlusion. *Invest Ophthalmol Vis Sci*. 2015; 56:3329–3336.
7. Dysli C, Wolf S, Hatz K, Zinkernagel MS. Fluorescence lifetime imaging in stargardt disease: potential marker for disease progression. *Invest Ophthalmol Vis Sci*. 2016;57:832–841.
8. Dysli C, Wolf S, Zinkernagel MS. Autofluorescence lifetimes in geographic atrophy in patients with age related macular degeneration. *Invest Ophthalmol Vis Sci*. 2016;57:2479–2487.
9. Sauer L, Schweitzer D, Ramm L, Augsten R, Hammer M, Peters S. Impact of macular pigment on fundus autofluorescence lifetimes. *Invest Ophthalmol Vis Sci*. 2015;56:4668–4679.
10. Schmidt J, Peters S, Sauer L, et al. Fundus autofluorescence lifetimes are increased in non-proliferative diabetic retinopathy [published online ahead of print August 13, 2016]. *Acta Ophthalmol*. doi:10.1111/aos.13174.
11. Schweitzer D, Schenke S, Hammer M, et al. Towards metabolic mapping of the human retina. *Microsc Res Tech*. 2007;70:410–419.
12. Schweitzer D. Metabolic mapping. In: Holz FG, Spaide RF, eds. *Medical Retina, Essentials in Ophthalmology*. Berlin: Springer; 2010:107–123.
13. Schweitzer D, Hammer M, Schweitzer F, et al. In vivo measurement of time-resolved autofluorescence at the human fundus. *J Biomed Opt*. 2004;9:1214–1222.
14. Early treatment diabetic retinopathy study design and baseline patient characteristics. ETDRS report number 7. *Ophthalmology*. 1991;98:741–756.
15. International Electrotechnical Commission (IEC). *International Standard 60825-1:2007* (Edition 2, ISBN 2-8318-9085-3)/ 60825-1:2014 (Edition 3, ISBN 978-2-8322-1499-2). International Electrotechnical Commission, TC 76, ICS 13.110, ICS 31.260.
16. Dysli C, Quellec G, Abegg M, et al. Quantitative analysis of fluorescence lifetime measurements of the macula using the fluorescence lifetime imaging ophthalmoscope in healthy subjects. *Invest Ophthalmol Vis Sci*. 2014;55:2106–2113.
17. Yehoshua Z, Rosenfeld PJ, Gregori G, et al. Progression of geographic atrophy in age-related macular degeneration imaged with spectral domain optical coherence tomography. *Ophthalmology*. 2011;118:679–686.
18. Morgan JI, Han G, Klinman E, et al. High-resolution adaptive optics retinal imaging of cellular structure in choroideremia. *Invest Ophthalmol Vis Sci*. 2014;55:6381–6397.
19. Loguinova MY, Zagidullin VE, Feldman TB, et al. Spectral characteristics of fluorophores formed via interaction between all-trans-retinal with rhodopsin and lipids in photoreceptor membrane of retina rod outer segments. *Biochemistry (Mosc)*. 2009;3:134–143.
20. Sparrow JR, Marsiglia M, Allikmets R, et al. Flecks in recessive Stargardt disease: short-wavelength autofluorescence, near-infrared autofluorescence, and optical coherence tomography. *Invest Ophthalmol Vis Sci*. 2015;56:5029–5039.
21. Sparrow JR, Fishkin N, Zhou J, et al. A2E, a byproduct of the visual cycle. *Vision Res*. 2003;43:2983–2990.
22. Secondi R, Kong J, Blonska AM, Staurenghi G, Sparrow JR. Fundus autofluorescence findings in a mouse model of retinal detachment. *Invest Ophthalmol Vis Sci*. 2012;53:5190–5197.
23. Duncan JL, Aleman TS, Gardner LM, et al. Macular pigment and lutein supplementation in choroideremia. *Exp Eye Res*. 2002;74:371–381.
24. Schweitzer D, Gaillard ER, Dillon J, et al. Time-resolved autofluorescence imaging of human donor retina tissue from donors with significant extramacular drusen. *Invest Ophthalmol Vis Sci*. 2012;53:3376–3386.
25. MacLaren RE, Groppe M, Barnard AR, et al. Retinal gene therapy in patients with choroideremia: initial findings from a phase 1/2 clinical trial. *Lancet*. 2014;383:1129–1137.

Investigative Ophthalmology & Visual Science